ISSN 3083-7219 (Print), ISSN 3083-7227 (Online)
Теорія і практика металургії, 2026, № 1
Theory and Practice of Metallurgy, 2026, No. 1

https://doi.org/10.15802/tpm.1.2026.01

UDC 669.15'74-198:669.046.5:536.7

Gasik M. M.

Thermodynamic equilibrium of high-carbon ferromanganese smelting

ORCID: 0000-0002-5782-7987. Aalto University Foundation, Espoo, Finland
Email: michael.gasik@aalto.fi

Гасик М. М.

Термодинамічна рівновага процесу виплавки високовуглецевого феромарганцю

ORCID: 0000-0002-5782-7987. Університетська Фундація Аалто, Еспоо, Фінляндія
Email: michael.gasik@aalto.fi

Abstract. *The goal of this study is to carry our detailed thermodynamic analysis of FeMn fluxless smelting process in submerged arc furnaces (SAF) using realistic plant data and compare the calculation results with industrial outcomes. Modern thermodynamic databases FactSAGE was deployed to assess equilibria inside separate phases and between them at 1400-1800°C for two FeMn78 alloys with different phosphorus content. Phases (metal, slag and gas) compositions were calculated with metal recovery value for manganese as well as through-recovery of manganese in both working slag and metal. It was found that temperature of the process 1500-1525°C predicts maximal recovery of manganese into the alloy. The outcomes allowed combination of blended manganese agglomerates, ores, return tails to be efficiently composed and converted into materials streams, which can be fed into the thermodynamic calculations. Such approach allows flexibility to optimize different scenarios in high-carbon ferromanganese fluxless smelting. The correlation of the calculations with industrial plant outcomes was found to be very good. The method gives a good basis to check behavior of different components and elements in the furnace, distribution of them between the phases (gas, metal, slag) and identify the pathways for improvement of the process leading to higher yield and quality. With the same thermodynamic database parameter similar approach can be used for other manganese ferroalloys.*
Keywords: *ferromanganese, thermodynamics, slag, metal, equilibria, metal recovery.*

Анотація. *Задачею роботи було проведення термодинамічного аналізу процесу виплавки високовуглецевого феромарганцю безфлюсовим методом у дугових печах з використанням реальних заводських даних і порівняння їх з результатами. Сучасна термодинамічна база даних FactSAGE була застосована для розрахунків рівноваги окремих фаз і між фазами в інтервалі температур 1400-1800°C для двох типів феромарганцю ФМн78 з різним вмістом фосфору. Склад окремих фаз і загалом всій системи було розраховано разом з виходом металу (прямого вилучення марганцю у стоп) і повного вилучення марганцю (металева і шлакова фази разом). Оптимальну температуру процесу було визначено у 1500-1525°C коли вилучення марганцю у металеву фазу максимальне. Процес розрахунку дозволяє комбінувати різні суміші агломератів, руд, хвостів і зворотних матеріалів для реалізації різних сценаріїв при виробництві феромарганцю. Отримані результати показали дуже добру кореляцію із даними заводського виробництва феромарганцю зокрема у хімічному складі металу, прямого і загального вилучення марганцю. Метод таким чином дозволяє оцінку поведінки різних компонентів і елементів у печі, їх розподіл між фазами (газ, метал, шлак) і визначення шляхів покращення процесу щодо виходу металу і його якості. Така ж сама база термодинамічних даних може бути застосована і для оптимізації інших марганцевих феросплавів. Дана робота демонструє, що коректне використання термодинамічних баз даних дозволяє зробити досить вірну оцінку характеристик процесу і якості феросплаву. Такі розрахунки ефективно заміняють спрощені калькуляції балансу шихти і енергії, даючи гнучкість у оптимізації феросплавного виробництва.*
Ключові слова: *феромарганець, термодинаміка, шлак, метал, рівновага, вихід металу.*

Introduction. Manganese-based ferroalloys such as ferromanganese (FeMn) and silicomanganese (FeSiMn) are essential components of modern steelmaking [1-3]. They are commercially produced by the carbothermic reduction of manganese oxide ores in submerged arc furnaces (SAFs) having in three-phase submerged arc furnaces, which have a three-electrode (Søderberg or self-baking type) circular or a six-electrode rectangular geometry, rated from about 20 to 90 MVA power capacity [1-4]. High carbon ferromanganese, one of the most used ferroalloy, typically contains around 72-82% Mn and 6-7% C, balance being Fe, Si and impurities. As in other ferroalloys, phosphorus is such an impurity which needs to be carefully controlled due to its negative impact in steelmaking [3, 5].

Literature analysis. A typical charge for FeMn production is composed of manganese ores, concen-

trates, agglomerates and returned tails depending on the quality of these raw materials - blending Mn-sources from different origins is a common practice for instance, to obtain a specific Mn/Fe ratio in the metal and limited phosphorus content [1, 3, 5, 6]. Manganese ores with a high content of phosphorus (0.18–0.22%) cannot be usually enriched by mechanical methods with simultaneous phosphorus removal and it passes into manganese concentrates, agglomerates – and finally into the alloy, decreasing its quality [1, 2, 7]. Ukrainian standard DSTU 3547-97 limits phosphorus content in high-carbon FeMn78 alloy to 0.10% (grade A) and 0.70% (grade B) [6].

Fluxes (dolomite, limestone) and carbonaceous agents (coke) and reusable waste (where applicable) are added according to expected desired composition of the alloy and the slag. These basic fluxes are commonly added to give the slag suitable chemical properties, smelting temperature, and viscosity to secure good furnace operation and a high manganese yield [3, 5]. High-carbon ferromanganese FeMn78 is commonly produced essentially by a flux-less process, which is more cost-effective over flux process [1, 3]. The resulting high-manganese slag (>35% Mn) is used at the next stage as the raw material in the charge for smelting silicomanganese with lower phosphorus content, which increases the through-recovery of manganese [1, 3, 5]. It is known that the phosphorus capacity of slags in this process is much depending not only on slag and metal compositions but also gas phase such as oxygen potential [8, 9]. Interactions between the slag, metal and gas phase are rather complex inside the SAF, depending on the location, temperature zones distribution and reaction and transport kinetics [10, 11]. Ferromanganese smelting practice therefore has accumulated engineering parameters linked to the core reactions of MnO reduction as the leading targeted force in the process [12].

Because many parameters of the smelting are not under direct observation, thermodynamic modeling was used to predict the process, mass and energy balances, and to correlate them with the experimental data. Earlier studies have used simplified schematics based on regular solution models [13]. This approach has limitations coming from the solution model itself as well as from the lack of parameters counting for multi-phase equilibrium. Later modeling was extended for application of thermodynamic databases allowed differences in mineral phase composition and specific interactions beyond the regular solution [14]. Also, recently a similar thermodynamic analysis to produce high-carbon FeMn using a SAF process was compared with the plant operation conditions to obtain a simplified simulation model [15]. Whereas being more detailed, this model was eventually limited to one temperature (1400°C) and charge composition. Such conditions are sufficiently replicable in the lab, but they do not reflect industrial practice.

Objectives of this work. The goal of this study is to carry out detailed thermodynamic analysis of FeMn smelting process using realistic plant data and compare the calculation results with industrial outcomes. If the correlation is sufficient, this gives a good basis to check behavior of different components and elements in the furnace, distribution of them between the phases (gas, metal, slag) and identify the pathways for improvement of the process leading to high yield and quality.

Materials and methods. For calculations of the expected equilibria in the conditions of a SAF the following assumptions have been made. First, only the thermodynamic equilibrium is considered, without kinetics of the process which imposes an ideally mixed reactor model. The temperature range was selected as 1400-1800°C and 1 atm of total pressure as it is typical for FeMn smelting. Charge materials mineral compositions (Table 1) were converted into oxides, including those minerals present in coke ash, and the sum of oxides was normalized to 100% (Table 2). One exception was done for phosphorus – it was entered into calculations as apatite $Ca_3(PO_4)_2$ because using P_2O_5 as a starting compound lead to immediate removal of all phosphorus into gas phase. Volatile sulfur and moisture were ignored, and losses-on-heating (LOH) were assumed to be only due to presence of carbonates (when all CO_2 is converted to the gas phase before melting but remained in the system). The composition of the briquettes from returns was approximated by 'diluted' ferromanganese adjusted to the experimental composition provided from the plant lab. Finally, the slag-metal waste (SMW) was represented by a mixture of ferromanganese scrap with RMS – re-workable manganese slag [1, 3] (Table 1).

Four phases considered in these calculations are gas, liquid metal, slag (with oxides originating from the coke ash) and – at the entry – coke as carbonaceous reducing agent. Possible transfer of materials from the electrodes (carbon) and lining (oxides) was neglected. For these phases the activity parameters were used if known, and otherwise an approximation has been deployed (the gas is also assumed to be ideal, and dust contribution was not counted).

The reaction between these phases was without restrictions on the transfer of elements from phase to phase (i.e., free mass exchange between all phases is assumed). Each analogous component (oxide or element) of the charge is combined (ore and non-ore components, Table 1) and converted into oxides and elements, Table 2. Phases (oxide, metal, gas) are first brought to equilibrium separately, assuming no interaction between them (i.e. testing for stability and the formation of metastable phases and immiscibility zones). After local phase equilibrium was calculated, all these phases are mixed as 4 streams at a constant temperature for calculations of the total equilibrium. In this work, thermodynamic software 'FactSAGE 6.0' (GTT Technologies GmbH, Germany) was used with the standard '*FToxid*' (slag melt database) and author's own '*OptiDB09*' metal melt database with optimized thermodynamic interaction parameters. Calculated data were obtained in tabulated form and as plots shown below.

Results. Numerical example for 1600°C for FeMn78P20 alloy is shown in Table 3. The total weight of all phases will be 3,310.8 kg (the initial mass in Table 2 is 3328 kg), i.e., with a discrepancy of only 0.52%. In this case, the coke carbon is completely consumed by reduction. The total mass of all components is 77800 mol, with a calculated enthalpy change of +114.48 kJ/mol, entropy of +78.72 kJ/mol, and free energy change of -51.637 kJ/mol (as it is negative it reflects the smelting process is thermodynamically favorable).

Figure 1 displays weight composition of the equilibrium gas phase (only major constituents shown). It is seen that whilst CO is the leading compound (as expected), transfer of manganese into gas phase is significant over 1500°C. At higher temperatures 1700-1800°C there is also increase of SiO and Mg(gas), but there is not much phosphorus compared to other species (note logarithmic scale).

Figure 2 shows components of the slag phase, reflecting the dominance of MnO and SiO_2 as major constituents, with the maximal MnO content to be reached around 1600°C. Increasing temperature lowers MnO content in the slag, but it does not improves Mn extraction into the metal phase (Fig. 3) - rather it accelerates manganese losses to the gas phase, decrease in C and an increase in Si in the alloy. Noteworthy, the mass of silicon in the metal changes only slightly at higher temperatures, but due to Mn evaporation losses, its mass fraction increases. Similar tendencies are also seen for FeMn78P70 alloy composition.

Discussion. The recovery of manganese into the metal and overall (through) one have been calculated as ratios of Mn in metal to total manganese input in the system, and respectively for Mn in metal and slag vs. total entered manganese (Fig. 4 for both alloys). There are slight differences related to various input compositions (for FeMn78P70 there was more MnO in the raw materials), but the trends are similar.

Table 1. Used original raw materials compositions including blended ores and agglomerates for smelting of ferromanganese.

Raw materials	**SiO_2**	**CaO**	**MgO**	**P**	**Al_2O_3**	**MnO**	**P_2O_5**	**Fe_2O_3**	**$MnCO_3$**	**$CaCO_3$**	**C**	**Si**	**Fe**	**Mn**
Agglomerates														
AMNV-1	15	4.4	1.2		3	64.8	0.490	3.86						
AMNV-2	26.1	8	2.4		3	50.0	0.420	3.14						
AMNV-1A	10.1	3.6	0.7		3	65.4	0.327	5.43						
AMNV-2П	21.8	10.1	5.1		3	50.1	0.233	2.86						
Mn ores														
KK48NZh	9.3	0.8	0.5		1.2	48.9	0.098	6.14	24.88	2.00				
KK28	13.6	6.3	4.8		2.1	0.5	0.152	1.71	57.94	15.75				
KK37	5.5	13.3	3.1		0.3	44.9	0.058	9.43	6.46	33.25				
Slags														
RMS	30.3	8.5	2.3		10.6	43.5	0.007	0.34						
Waste slag	50.3	16.8	5.1		7.9	15.0	0.140							
SMW	9.09	2.55	0.69	0.126	3.18	13.05					4.55	0.63	10.09	54.6
Coke 10% ash	5.14	1.41	0.22	1.67	1.28			1.75			85.46			
Limestone	1		1							98				
Iron ore	3.5	0.5	0.5		3.5			92						
Quarzite	97.8	0.5	0.2		1			0.5						
FeMn (0.18%P)											6.5	0.9	14.42	78

Table 2. Normalized raw materials input (kg) used in calculations. Note that initial gas phase (mainly CO_2) originates from the carbonate components decomposition.

Ferroalloy type:	**FeMn78P20**	**FeMn78P70**
Oxide phase (with coke ash oxides):		
SiO_2	307.708	389.123
CaO	45.826	106.311
MgO	18.271	27.969
Al_2O_3	63.121	93.097
MnO	1524.963	1804.059
P_2O_5	4.789	10.047
Fe_2O_3	169.616	239.358
$MnCO_3$	452.187	127.554
$CaCO_3$	36.347	10.253
Metal phase:		
Mn	256.130	256.130
Fe	47.351	47.351
P	0.591	0.591
Si	2.955	2.955
C	21.344	21.344
Coke: C solid	376.801	358.858
Total mass, kg	**3328**	**3495**

These data were compared with the real averaged ferroalloys plant numbers (Table 4). It is noteworthy that the calculated values surprisingly well match the plant data for Mn recovery, despite some differences in Si and C content, as well as the composition of the gas phase. Significant loss of manganese under industrial conditions is likely much compensated by Mn gas condensation or absorption in the layer of unreacted charge, where solid-phase reduction and accumulation of manganese in a new metallic phase can occur, subsequently entering the metal bath.

Table 3. Example for equilibrium at 1600°C for FeMn78P20 alloy (in % wt.; for slag phase shown in % mol.)

Phase	Mass/volume	Composition
Gas	32204 mol, 4950.2 m^3, 997.26 kg	88.99 CO, 10.963 Mn, $1.736\cdot10^{-2}$ CO_2, $1.61\cdot10^{-2}$ Mg, $1.21\cdot10^{-2}$ SiO, $3.71\cdot10^{-5}$ Fe, $2.26\cdot10^{-5}$ Ca, $4.4\cdot10^{-7}$ Al, $1.33\cdot10^{-7}$ Si, $9.72\cdot10^{-9}$ P, $8.45\cdot10^{-9}$ MgO, $1.75\cdot10^{-9}$ Al_2O, $1.63\cdot10^{-9}$ AlO, $2.43\cdot10^{-10}$ CaO, $6.57\cdot10^{-13}$ O_2
Metal	29126 mol, 1174.8 kg	14.128 Fe, 72.289 Mn, 0.233 P, 4.38 Si, 8.97 C
Slag	16740 mol, 1138.8 kg	2.67 MgO, $2.95\cdot10^{-4}$ FeO, 66.318 MnO, 20.25 SiO_2, 7.05 CaO, 3.7 Al_2O_3, $1.71\cdot10^{-7}$ Fe_2O_3, $9.77\cdot10^{-10}$ $Ca_3(PO_4)_2$, $7.9\cdot10^{-3}$ Mn_2O_3, $3.44\cdot10^{-4}$ SiC

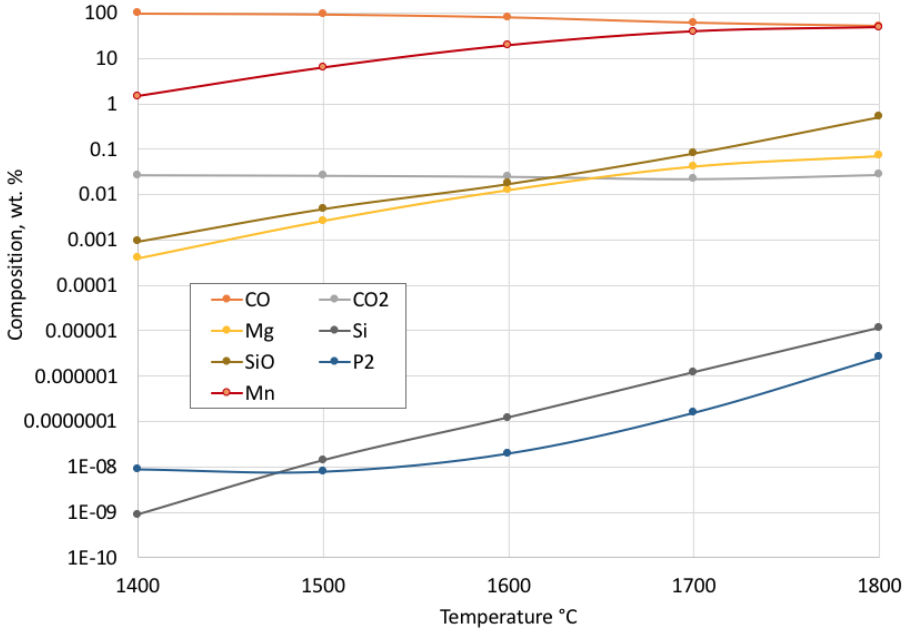

Fig. 1. Gas phase components for FeMn78P20 smelting at different temperatures.

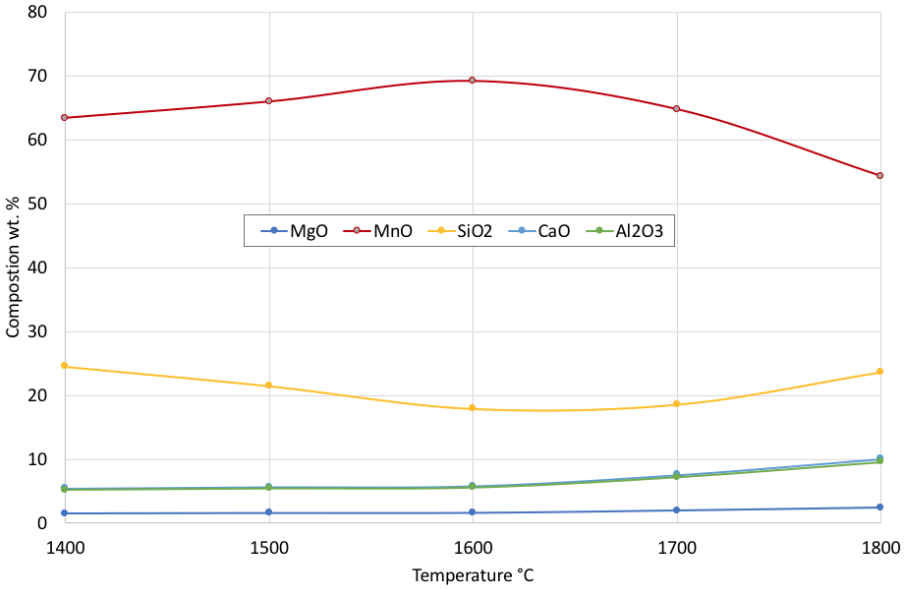

Fig. 2. Slag phase major components for FeMn78P20 at different temperatures.

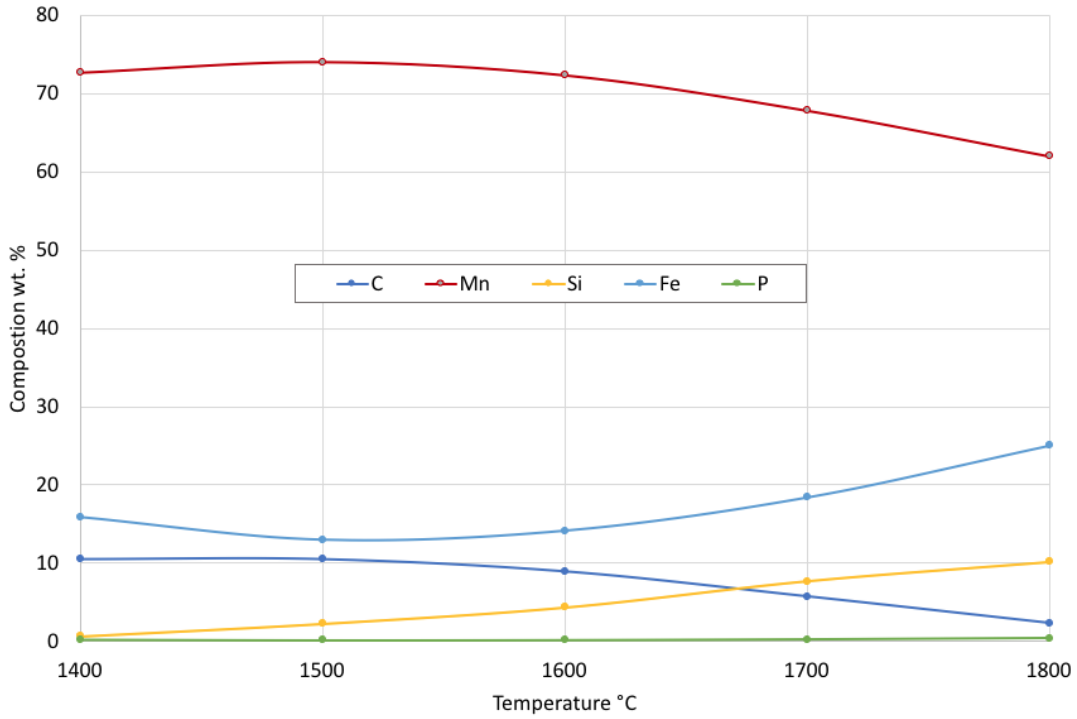

Fig. 3. Metal phase components for FeMn78P20 smelting at different temperatures.

Table 4. Comparison of calculated and experimental plant data.

Parameter	C	Si	Mn	P	Fe	Mn recovery into metal	FeMn yield, kg	Slag yield, kg/t alloy
FeMn78P20								
Calculated:	7.3	1.5	73.9	0.21	17.1	57.2	1161	1155
Plant data:	6.5	0.9	78.0	0.18	12.6	62.1	1000	1254
FeMn78P70								
Calculated:	6.8	2.3	72.6	0.39	17.9	60.0	1341	1100
Plant data:	6.1	1.9	78.6	0.41	14.5	60.2	1000	1540

If this correlation validity is accepted, one can estimate the expected temperatures of the smelting process when the manganese recovery is matched to the experimental data of Table 4. For Fig. 4 this leads to ~1525°C for FeMn78P20 and 1500-1520°C for FeMn78P70. The lower yield of the convertible manganese slag in calculations compared to the plant data (Table 4) is related to the expected higher metal yield. This could also be explained due to the higher recovery of silicon, iron, and carbon into the melt, which somewhat reduces the fraction of manganese.

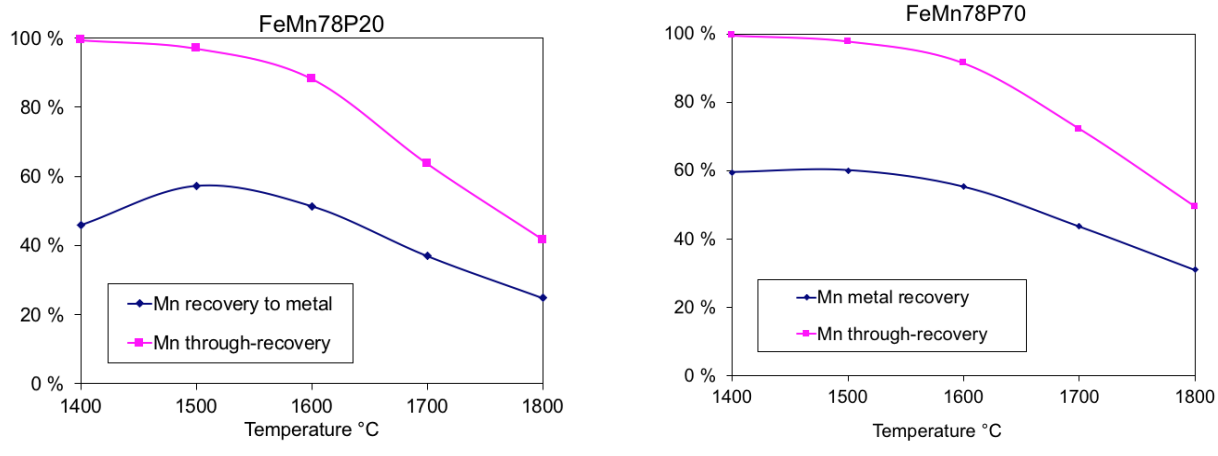

a b

Fig. 4. Manganese recovery calculated by thermodynamic equilibration at different temperatures for FeMn78P20 (a) and FeMn78P70 (b).

Conclusions. The results of calculations with updated thermodynamic data for ferromanganese smelting and their comparison with experimental (plant) values have demonstrated a very good correlation. They also show several variables that are hardly observed directly in industrial practice (e.g. expected temperature in the reaction zone or immediate gas phase composition). Equilibration predicts a higher degree of carbon and silicon conversion into the metal and virtually almost complete removal of phosphorus from the slag in this fluxless process. Significant manganese loss at elevated temperatures and negligible phosphorus loss were predicted but they could not be directly confirmed with experimental data. Very low concentrations of high-oxidation oxides (Fe_2O_3, Mn_2O_3) and SiC in the slag are consistent with literature and experimental practice. If manganese recovery is taken as a target feature parameter, average temperature of 1500-1525°C looks being an optimal range for this process, as further temperature increase will lead to more manganese losses. This range is higher than was previously analyzed 1400°C in alternative study [15].

Such calculations can be carried out excluding manganese as a component of the gas phase; however, to approximate the calculation to real conditions, a more accurate knowledge of air consumption as a reaction component is necessary (for example dilution of the gas phase with nitrogen can significantly shift the equilibrium of all reactions which involve gas products).

This work proves that careful assessment of input parameters and use of proper thermodynamic databases are valuable tools for estimation of the process features and resulting products quality, which could help smelting plants to manage better production. Embedded thermodynamic calculations are efficiently replacing manually set calculation procedures [3] or simplified models [13] for charge and energy demands in the process without assumptions for losses or phase partition.

References

1. Gasik, M. I. (1992). *Manganese*. Metallurgya
2. Gasik, M. I., Lyakishev, N. P., & Gasik, M. M. (2009). *Physical chemistry and technology of ferroalloys*. Sistemnye Technologii
3. Gasik, M. I., Dashevskii, V. Ya., & Bizhanov A. (2020). *Ferroalloys Theory and Practice.* Springer, Cham (Switzerland). https://doi.org/10.1007/978-3-030-57502-1
4. Gladkikh, V. A., Gasik, M. I., Ovcharuk, V. N., & Proydak, Yu. S. (2007). Ferroalloy electric furnaces. System Technologies
5. Olsen, S., Tangstad M., & Lindstad T. (2007). *Production of manganese ferroalloys*. Tapir Forlag
6. Velichko, B. F., Gavrilov, V. A., Gasik, M. I., et al. (1996). *Metallurgy of manganese of Ukraine*. Technika
7. Gvelisiani, G. G., Baratashvili, I. B., & Tsagareishvili, D. Sh. (1982). *Thermodynamics of the interaction of manganese with phosphorus.* Metsniereba
8. Maramba, B., & Eric, R. H. (2008). Phosphide capacities of ferromanganese smelting slags. Minerals Engin. 21, 132–137. https://doi.org/10.1016/j.mineng.2007.07.012
9. Yuanchi, D., Shangxing, G., & Chen, E. (1997). Control of oxygen potential and its effect on dephosphorization in ferromanganese. In: Proc. Eighth Intern. Ferroalloy Congr. INFACON 8, Bejing, China, 255–258
10. Shaojun, C., & Kuangdi, X. (2023). Ferromanganese. In: Xu, K. (eds) ECPH Encyclopedia Mining & Metallurgy. Springer, Singapore. https://doi.org/10.1007/978-981-19-0740-1_1023-1
11. Lee, Y. E., & Kolbeinsen, L. (2021). Behavior of slag in ferromanganese and silicomanganese smelting process. *Metall. Mater. Trans B*52, 3142–3150. https://doi.org/10.1007/s11663-021-02242-2
12. Coetsee, T. (2018) MnO reduction in high carbon ferromanganese production: practice and theory. *Miner. Process. Extr. Metall. Rev*., 39, 351–358. https://doi.org/10.1080/08827508.2018.1459618
13. Li, H., Morris, A. E., & Robertson, D. G. C. (1998). Thermodynamic model for MnO-containing slags and gas-slag-metal equilibrium in ferromanganese smelting. Metallurgical and Materials Transactions B, 29(6), 1181–1191. https://doi.org/10.1007/s11663-998-0040-z
14. Kutsyn, V. S., Gasik, M. M., & Gasik, M. I. (2012). Thermodynamic computer modeling of phase transformations in complex oxide systems, equivalent to manganese agglomerates made by existing and developed technologies. *Metall. Mining Ind*., 4(3), 16–24
15. Nam, J., van Ende, M-A., & Jung, I. H. (2022). Ferromanganese production in a submerged arc furnace: thermodynamic and energy balance analysis. *JOM*, 74(4), 1624-1632. https://doi.org/10.1007/s11837-021-05121-y

Надіслано до редакції / Received: 02.01.2026
Прорецензовано / Peer-Reviewed: 14.02.2026
Прийнято до друку / Accepted: 16.03.2026
Опубліковано / Published: 30.03.2026